Ultra Wideband Indoor Radio Channel Models: Preliminary Results

Veikko Hovinen, Matti Hämäläinen, Timo Pätsi

Centre for Wireless Communications, P.O. Box 4500
FIN-90014 University of Oulu, FINLAND
email: veikko.hovinen@ee.oulu.fi

ABSTRACT

Knowledge of the signal propagation mechanisms in the channel is vital for the radio system design and the system performance analysis. However, currently published wideband or narrowband radio channel models do not offer spatial resolution high enough for the ultra wideband (UWB) applications and the real channel measurements are needed. In this paper is given the preliminary UWB radio channel model for a selected radio link configuration in indoor environment.

1. INTRODUCTION

Ultra wideband (UWB) transmission techniques utilize extremely wide propagating radio signal bandwidth [1]. This allows one to use UWB technology in different kinds of applications that demand very accurate temporal or spatial resolutions. The applications can be, for example, indoor positioning systems or radar applications as well as high data rate communication links. The most important benefits of the UWB technology are good penetration capability combined with high accuracy. Low transmission power and large bandwidth make the power spectral density of the transmitted signal extremely low, which might allow UWB applications to use same frequency bands as the existing radio systems are using (overlay technique).

Knowledge of the signal propagation mechanism in the channel is vital for the radio system design and the system performance analysis. However, currently published radio channel models do not offer delay resolution high enough for the UWB applications. The existing radio channel models are generated using about 10 MHz to about 100 MHz bandwidths. This is why the specific UWB radio channel models are needed to characterize the radio channel with the bandwidth larger than 1 GHz. In our study the indoor radio channel sounding was carried out using frequency sweeping method. In post-processing the recorded radio channel frequency responses are inverse Fourier transformed to achieve channel impulse responses (averaged to delay profiles). Finally, the channel characterization and the statistical radio channel models are generated from the impulse responses.

This paper is organized as follows. Chapter 2 introduces the radio channel measurement technique and the setup used in this study. Chapter 3 introduces the environments where the measurements have been performed. The data pre-processing procedure is explained in Chapter 4. The preliminary radio channel models are given in Chapter 5 and, finally, the conclusion in Chapter 6.

2. ULTRA WIDEBAND RADIO CHANNEL MEASUREMENT TECHNIQUES

To gain knowledge of the UWB radio channel, there are two possible ways to perform the channel sounding. Channel can be measured in frequency domain using a frequency sweep technique. The other method is a time domain measurement that is based on the impulse transmission. In the former technique, a wide frequency band is swept using a set of narrowband signals, and the channel frequency response is recorded using a vector network analyzer. This corresponds to conventional S_{21}-parameter measurement setup, where the device under test (DUT) is a radio channel. In the latter case, a narrow pulse is sent to channel and the channel impulse response is measured using a digital sampling oscilloscope. The corresponding train of impulses can also be generated using a direct sequence spread spectrum based measurement system with a correlation receiver that is widely used in wideband radio channel modeling. The drawback in this technique is the need of very high chip rates to achieve bandwidths of several GHz.

2.1. Measurement Setup

In our study, the frequency domain measurement system was selected. The RF signal is generated and received by the network analyzer, which simplifies the measurement setup. Frequency domain approach also makes it possible to use wideband antennas, instead of special impulse radiating antennas. The physical indoor environment during the sounding was kept as static as possible, but no effort was made to control the radio interference from the other RF sources.

The sounding system consists of an Agilent 8720ES vector network analyzer [2], an Agilent 83017A wideband amplifier [3], a conical antenna pair, and a control computer with a LabVIEW software. The network analyzer is operated in response measurement mode. An external amplifier is connected to analyzer's transmitter port to increase the transmitted power level. The antennas used in the measurements are CMA-118/A conical antennas by Antenna Research Associates, Inc [4]. Conical antennas have omni-directional radiation pattern and constant phase center, the features that are important in the wideband radio channel sounding. Table 1 lists the main parameters of the measurements. The given antenna gain is specified by the antenna manufacturer. The block diagram of the used measurement setup is presented in Fig. 1. The figure explains also the main features of a post-processing procedure. The measurement setup is described in more detail in [5].

0-7803-7496-7/02/$17.00 ©2002 IEEE. 2002 IEEE Conference on Ultra Wideband Systems and Technologies

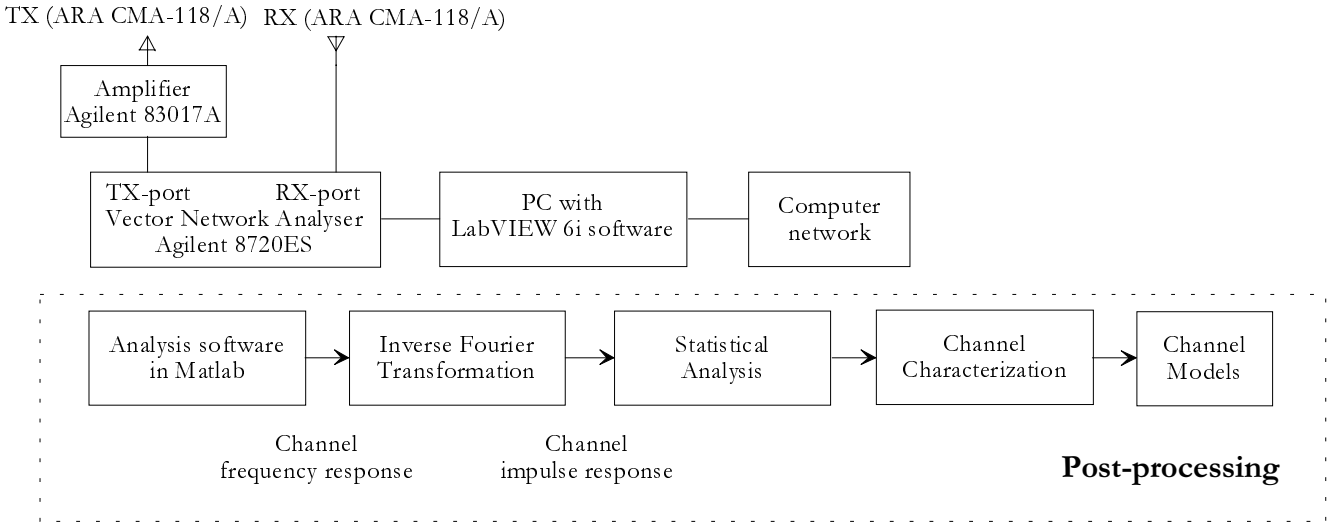

Figure 1. *The radio channel measurement setup used in the study.*

Dynamic range mentioned in Table 1 is reduced to the output of the RX antenna. Specified dynamic range for the network analyzer is 100 dB [2] but the cable losses diminished about 20 decibels of that range.

Table 1. Measurement setup parameters.

Parameter	Value
Frequency band	2 to 8 GHz
Bandwidth (frequency span)	6 GHz
Number of points over the band	1601
Sweep time	800 ms
Dynamic range	80 dB
Average noise floor	-120 dBm
Transmitted power @ 2 GHz	+ 10 dBm ± 1 dB
Amplifier gain	36 dB ± 1 dB
Antenna gain	0 dBi (typical)

Upper bound limit for the detectable delay of the channel in time domain, τ_{max}, can be defined by the number of frequency points per a sweep and the used bandwidth B (frequency span) as [2]

$$\tau_{max} = (\text{number of points} - 1)/ B. \quad (1)$$

Using the parameter values from Table 1, Eq. (1) yields 1600/(6 GHz) = 266.6 ns that corresponds to 80 m, which is quite reasonable value for the indoor environments.

In frequency sweep mode the sounding signal is rapidly swept through the whole band of interest. Long propagation delay in the channel will cause the receiver to sample at a frequency that is a bit higher than the received frequency at the antenna input. This frequency shift Δf is a function of the propagation time t_{tr} (time of flight), the frequency span B and the sweep time t_{sw} as [6]

$$\Delta f = t_{tr}\left(\frac{B}{t_{sw}}\right). \quad (2)$$

Δf has to be smaller than IF bandwidth of the analyzer. Using the sweep time from Table 1, span B = 6 GHz and 3 kHz IF bandwidth, Eq. (2) yields maximum signal flight time 400 ns.

3. MEASUREMENT ENVIRONMENTS

The indoor UWB radio channel measurements have been performed at the main building of the University of Oulu, using different types and various sizes of rooms.

The idea of the measurements was to set the TX-antenna into the middle of the room and to move the RX-antenna to several positions. To get reliable channel models the sweep time should not exceed the coherence time of the channel. In our study, the frequency response at each antenna position has been recorded with three antenna heights in both ends. This gives altogether nine (3∗3) transmission links for each RX-position. For statistical averaging, the frequency band was swept and recorded 500 times for each link. Sweep time of the measurement system is 800 ms, and recording 500 sweeps takes typically 1990 seconds. All movements inside the room were frozen during the recording time. The transmissions of the other radio systems cannot be suppressed during the recordings. However, the measured frequency band is above the bandwidths of broadcasting networks, cellular and other commonly used radio systems, which means that the influence of the interfering systems is negligible.

Results shown in this paper have been calculated for antenna heights H_{TX} = 2.2 m and H_{RX} = 1.1 m, and vice versa. The distances between TX-antenna and RX-antenna (length of the transmission link) in this data set were between 1.25 m and 8.10 m, which corresponds to initial propagation delays from 4.2 ns to 27.0 ns. The first measurement campaign covered the situations where the transmitting and receiving antennas were

located in the same room. Both the line-of-sight (LOS) and non-LOS links were studied. The research will continue with the measurements where TX-antenna and RX-antenna will be in the different rooms (through-wall measurement).

4. DATA POST-PROCESSING

The amplitude response data were converted into Matlab format and inverse Fourier transformed into delay domain. A Hanning window was applied before transformation to make it easier to locate line-of-sight component of the signal. The data was simultaneously transformed into delay domain using no windowing.

The system noise level was estimated from absolute delay range 0 ns — 3 ns, and was found to be around –105 dBm limiting the dynamic range typically to 40 dB. The time of arrival (TOA, initial delay) of the LOS component was extracted for each of the radio links using the average delay profile of 500 impulse responses (small-scale statistics). Initial delay was removed from the results, and the statistical parameters were extracted from this data.

Maximum excess delay was limited to 70 ns, which corresponds to 420 samples in delay domain. The limit was found by removing the strongest reflections and plotting average delay profiles from various data sets. This corresponds to large-scale statistics represented in Fig 2, where the reflections are plotted in red (dark gray shade).

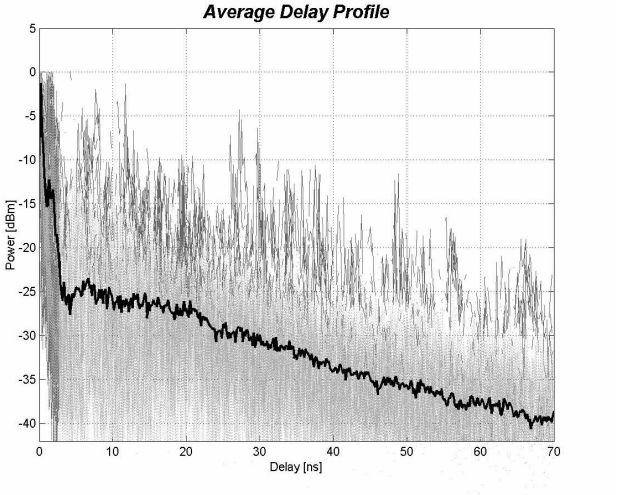

Figure 2. Average delay profile (32500 impulse responses).

5. RADIO CHANNEL MODELS

A discrete model for a time-variant fading multipath channel is

$$h(t) = \sum_n a_n(t)\, s(t - \tau_n(t)), \qquad (3)$$

where $s(t)$ is the transmitted signal, $a_n(t)$ is the amplitude gain of the n^{th} multipath channel and $\tau_n(t)$ is the corresponding excess delay. In indoor environment with no moving scatterers and with fixed antenna positions $a_n(t)$ and $\tau_n(t)$ are assumed to be constant during the observation time. Measurements recorded in various antenna positions give an estimate of the average static indoor channel. Movement of scatterers or altering the length of radio link will introduce Doppler shift, which in turn reduces the coherence time t_{coh} of the channel. The channel can be measured, if the measurement time is shorter than the coherence time. This assumption is valid in static indoor measurements.

A multipath channel is typically modeled as a linear tapped delay line (a FIR filter), with complex tap coefficients [7]. In computer simulation the time variance of the channel filter is realized in various ways, the simplest and most straightforward being a FIR filter, whose coefficients are updated from previously stored complex-valued channel data. The drawback of this approach is the limited randomness, since eventually the data have to be re-used. Statistical channel description gives more freedom for simulation. In the tapped delay line model the time variation is realized by mixing the multiplicative white noise through a bandpass filter directly to the tap coefficients.

Nevertheless, a realistic assumption for a static indoor channel is a Rician fading model. Rician fading signals have amplitude $a_n(t)$ that is distributed according to [8]

$$p_R(a) = \frac{a}{\sigma^2} \exp\left(-\frac{a^2 + s^2}{2\sigma^2} \right) I_0\left(\frac{as}{\sigma^2} \right), a \geq 0, \qquad (4)$$

where σ is the standard deviation and I_0 is the zeroth order modified Bessel function of the first kind. The non-centrality parameter s is defined by [8]

$$s^2 = \left\| \bar{a}(t) \right\|^2, \qquad (5)$$

where $\bar{a}$ is mean complex amplitude.

Signal-to-noise ratio (SNR) of a Rician fading signal is defined as

$$k = \frac{s^2}{2\sigma^2} = \frac{s^2}{\eta^2}, \qquad (6a)$$

which in logarithmic scale is

$$k = s_{dB}^2 - \eta_{dB}^2. \qquad (6b)$$

Rayleigh fading channel is a special case of Rician channel with $k = 0$. It has been shown [9] that the Rician fading channel becomes effectively Rayleigh fading when k becomes smaller than 5 dB.

A large scale (long-term) model is constructed from data that has been collected in various locations. Because antenna positions and room sizes vary, we need to separate pure reflections from the random part of the model. In other terms, the channel model contains a deterministic environment dependent ray-tracing part (DM) and a statistical environment independent Rician fading part (SM), as shown in Figure 3.

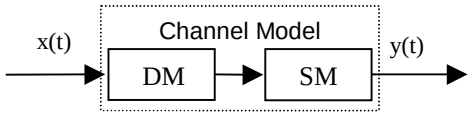

Figure 3. Channel Model.

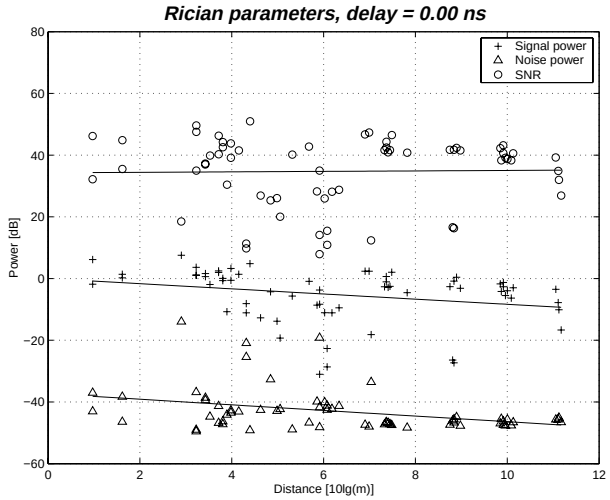

Figure 4. Rician parameters for line-of-sight path.

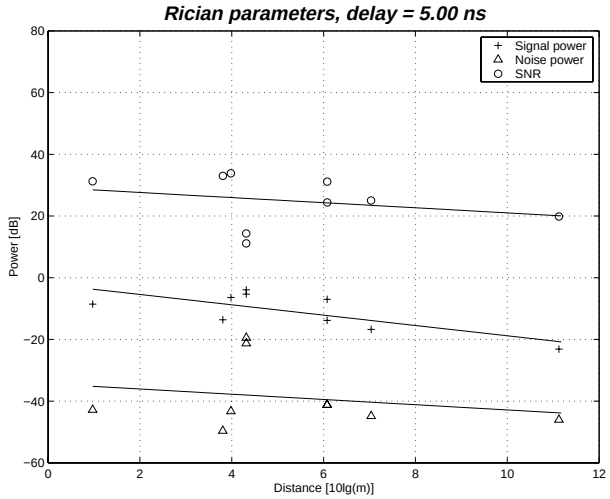

Figure 5. Rician parameters at delay 5 ns.

DM contains static reflections, whose delay and power estimates can be modeled either with ray tracing tools or calculated from a simplified reflection model. The power of the LOS signal is normalized to unity, and it is contained in the DM part.

Parameters for SM are extracted from the measurement data after normalizing to average power level and removing the most significant reflections. Figures 4 and 5 show the statistical parameters of SM as functions of antenna distance at delays 0 ns and 5 ns, respectively. A linear regression line $k(\tau, d) = a_{\mathrm{k}}(\tau)d + b_{\mathrm{k}}(\tau)$, d being the logarithmic antenna separation, can be fitted to the normalized logarithmic data. We notice that a_{k} is nearly zero within the observation distance range at LOS, but has value $a_{\mathrm{k}} = -1.67$ at delay 5 ns. In other words, k decreases exponentially in linear scale.

Estimates for $k(\tau,d)$ can be tabulated directly, but here we have expressed them using estimates of signal power $s^2(\tau,d)$ and noise power $h^2(\tau,d)$. Figures 6 and 7 show the values for regression parameters a_s, a_η and b_s, b_η as functions of excess delay. Again, we can fit piecewise linear regression lines to this data and get expressions

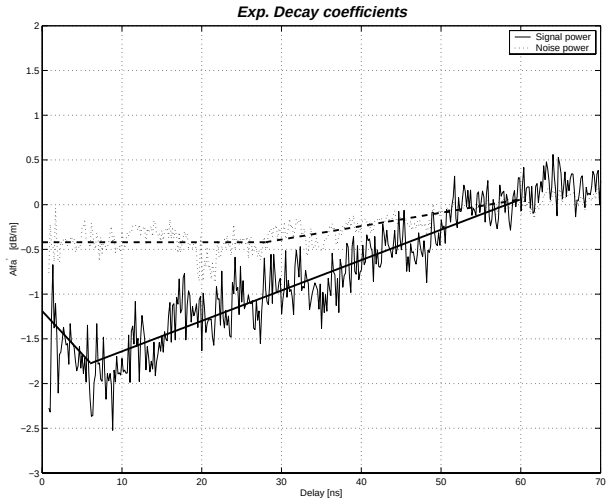

Figure 6. Coefficients a_s and a_η for exponential decay of Rician parameters.

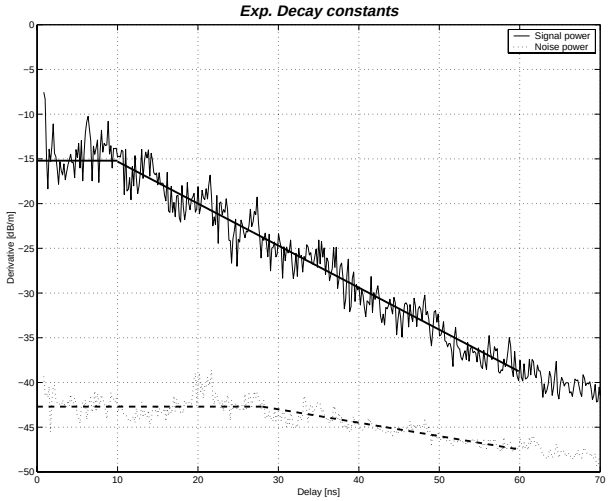

Figure 7. Constants b_s and b_η for exponential decay of Rician parameters.

$$a_{\mathrm{s}}(\tau) = \alpha_{\mathrm{s}}'\tau + \alpha_{\mathrm{s}} \tag{7a}$$

$$a_{\eta}(\tau) = \alpha_{\eta}'\tau + \alpha_{\eta} \tag{7b}$$

and

$$b_{\mathrm{s}}(\tau) = \beta_{\mathrm{s}}'\tau + \beta_{\mathrm{s}} \tag{8a}$$

$$b_{\eta}(\tau) = \beta_{\eta}'\tau + \beta_{\eta}\,. \tag{8b}$$

where subscripts s and η are associated to $s^2(d,\tau)$ and to $\eta^2(d,\tau)$, respectively. Tables 2 and 3 list the regression parameters for the signal power and the noise power.

Table 2. Parameters for Exponential Decay Coefficient α .

Delay range	Signal power		Delay range	Noise power	
τ	α'_S	α_S		α'_η	α_η
0-6 ns	-0.095	-1.20	0-28 ns	0.0	-0.42
6-60 ns	0.035	-1.98	28-60 ns	0.015	-0.84

Table 3. Parameters for Exponential Decay Constant β .

Delay range	Signal power		Delay range	Noise power	
τ	β'_S	β_S		β'_η	β_η
0-10 ns	0.00	-15.2	0-28 ns	0.00	-42.7
10-60 ns	-0.47	-10.6	28-60 ns	-0.15	-38.5

The signal power and the noise power can be expressed in compact matrix forms

$$\mathbf{S} = \mathbf{a}_S'^{T}\mathbf{d} + \mathbf{b}_S'^{T}, \quad (9a)$$

$$\mathbf{N} = \mathbf{a}_\eta'^{T}\mathbf{d} + \mathbf{b}_\eta'^{T}, \quad (9b)$$

where T denotes transpose operation, and dimensions of **a** and **b** are that of delay, and dimension of **d** is that of antenna separation. According to Eq. (6b) signal-to-noise ratios can be expressed as

$$\mathbf{K} = \mathbf{S} - \mathbf{N}. \quad (10)$$

Matrices **S**, **N** and **K** contain the signal power (delay profile), noise power and the SNR values for Rician fading channel, respectively. Each of the columns describes the fading statistics as a function of delay at the given antenna separation *d*. When **K** is below 5 dB, a Rayleigh channel with corresponding noise power applies [8].

The presented channel model can be applied to computer simulations for performance studies of UWB systems.

6. CONCLUSION

This paper explains the UWB indoor radio channel measurement campaign being carried out at the University of Oulu. The preliminary channel model for a selected radio link is presented. Further studies will complete the modeling of the radio channels for the radio links configurations that were not covered here.

The presented channel model can be applied to computer simulations of performance studies of UWB systems in short-range indoor situations with clear line-of-sight signal.

7. ACKNOWLEDGEMENTS

This work is funded by the National Technology Agency of Finland (Tekes), Nokia, Elektrobit and the Finnish Defence Forces. Authors would like to thank the sponsors for their support. Prof. Seppo Karhu and prof. Jari Iinatti are also appreciated for several discussions during the measurement and modeling process. M.Sc. (Tech.) student Niina Laine is appreciated for her assistance during the data post-processing.

8. REFERENCES

[1] Scholtz R.A., Win M.Z., "Impulse Radio", *Wireless Communications, TDMA versus CDMA* (Ed. Glisic S., Leppänen P.), Kluwer Academic Publisher, London 1997, pp. 245-263.

[2] Agilent 8720E Family, Microwave Vector Network Analyzers, Data sheet, Agilent Technologies.

[3] 83000A Series Microwave System Amplifiers, product overview, Agilent Technologies.

[4] http://www.ara-inc.com/

[5] Hämäläinen M., Pätsi T., Hovinen V., "Ultra Wideband Indoor Radio Channel Measurements," *Proc. of the 2nd Finnish Wireless Communication Workshop*, FWCW01, Tampere, Oct 23-24, 2001.

[6] Response from Agilent Technical Support

[7] Bello P. A., "Characterization of Randomly Time-Variant Linear Channels", IEEE Transactions on Communications Systems, Dec 1963

[8] Proakis J. G., Digital communications, McGraw-Hill, 1995

[9] Talvitie J., "Wideband Radio Channel Measurement, Characterisation and Modelling for Wireless Local Loop Applicatios," Ph.D. dissertation, Acta Universitatis Ouluensis Technica C99, Oulu, 1997.